On the modelling of spalling in plain concrete

Xiaowei Liu*, Chun Hean Lee, Peter Grassl

James Watt School of Engineering, University of Glasgow, Glasgow, UK
x.liu.7@research.gla.ac.uk, chunhean.Lee@glasgow.ac.uk, peter.grassl@glasgow.ac.uk

Abstract

When concrete is subjected to high strain rates due to dynamic loading, its strength will increase significantly compared to quasi-static loading. Here, we develop a constitutive model based on damage mechanics which can, on the one hand, predict the dependence of tensile strength on high strain rates, and, on the other hand, produce mesh independent numerical results using the crack band approach. A strain based scalar damage model is extended to dynamic loading by introducing a strain rate dependent damage history variable so that the onset of damage for high strain rates is delayed. To circumvent mesh dependency within the framework of the crack band approach, the damage evolution is formulated as a function of the displacement rate of the damaged element. The constitutive model is implemented in the finite element software OOFEM. Finally, the new model is assessed by applying it to a spall test based on a modified Split Hopkinson Bar experiment reported in the literature.

Key words: *High strain rate; Damage mechanics; Concrete; Fracture*

1 Introduction

Concrete structures subjected to extreme dynamic events, such as impact and explosion, exhibit failure processes in the form of crushing and spalling which differ significantly from those obtained from statically loaded structures [5]. The failure process of concrete structures under impact loads are very complex. Near the load point, the concrete is in the state of large compression deformation and high compressive strain rates. On the free boundary of the structure, the compressive stress waves are reflected to form tensile stress waves which cause spalling under high tensile strain rates [9]. For predicting the response of concrete structures, it is required to develop models which can capture the effect of high strain rates on strength and damage evolution of concrete in tension and at the same time provide mesh independent results.

One popular way of modelling cracking and damage evolution in concrete is by using stress-strain constitutive laws which exhibit strain softening. If strain softening is used directly within local constitutive models without any special techniques, the results in the form of load-displacement curves become mesh-dependent. If the mesh size is reduced, the dissipated energy will tend to zero. Multiple modelling strategies were proposed in the past to overcome this problem. In nonlocal and gradient models, the stress at a point is made dependent history variables at the point and its vicinity [1]. These models are powerful but require very fine meshes. An alternative approach is to make the softening part of the stress-strain curve mesh-dependent. For concrete, Bažant and Oh [2] introduced the crack-band model to overcome the issue with zero dissipation upon mesh-refinement. This modelling approach is numerically very efficient because it does not require very fine meshes [4]. The main aim of this study is to introduce strain rate dependence of tensile strength within the crack-band model for an isotropic damage model. We aim to achieve this by making the history variables used in the function of the damage variable dependent on the strain rate. This is inspired by models in which the onset of damage is delayed [8]. Once damage has been initiated, the damage evolution is modeled as a function of the displacement rate to avoid mesh dependence. The constitutive model is implemented in the open source finite element program OOFEM[7] and applied to the finite element analyses of modified Split Hopkinson Bar (SHB) epxeriments reported in [9].

2 Methodology

The isotropic damage model is based on the following stress-strain relationship:

$$\boldsymbol{\sigma} = (1-\omega)\,\bar{\boldsymbol{\sigma}} = (1-\omega)\,\mathbf{D}_{\mathrm{e}} : \boldsymbol{\varepsilon} \tag{1}$$

where $\mathbf{D}_{\mathrm{e}}$ is the elastic stiffness based on Young's modulus E and Poisson's ratio ν; $\bar{\boldsymbol{\sigma}}$ is the effective stress; tensor $\boldsymbol{\varepsilon}$ is the strain tensor and ω is the damage variable ranging from 0 (undamaged) to 1 (fully damaged).
The evolution of the damage variable is defined as

$$(1-\omega)\, E\kappa_1 = f_{\mathrm{t}} \exp\left(-\omega\kappa_2 h_{\mathrm{e}}/w_f\right) \tag{2}$$

for ω using the standard Newton-Raphson method. Where h_e is the characteristic element length, f_t is the tensile strength and w_{f} is the crack opening threshold in Figure 2. Furthermore, κ_1 and κ_2 are two strain rate dependent history variables which are defined as

$$\dot{\kappa}_1 = \dot{\kappa}/\alpha \text{ and } \dot{\kappa}_2 = \dot{\kappa}\alpha \tag{3}$$

Here, α is a rate dependent factor. Furthermore, κ is the maximum equivalent strain reached in history of the material. The expression of equivalent strain $\tilde{\varepsilon}$ is

$$\tilde{\varepsilon} = \frac{1}{E}\sqrt{\sum_{I=1}^{3} \langle\bar{\sigma}_{\mathrm{I}}\rangle^2} \tag{4}$$

where $\bar{\sigma}_{\mathrm{I}}$ are the principal values of the effective stress and $\langle\bar{\sigma}_{\mathrm{I}}\rangle$ are their positive parts. As shown in the Figure 1, this equivalent strain definition gives a modified Rankine strength envelope at the onset of damage ($\tilde{\varepsilon} = f_{\mathrm{t}}/E$).

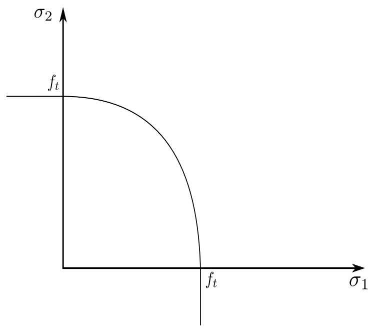

Figure 1: Strength envelope.

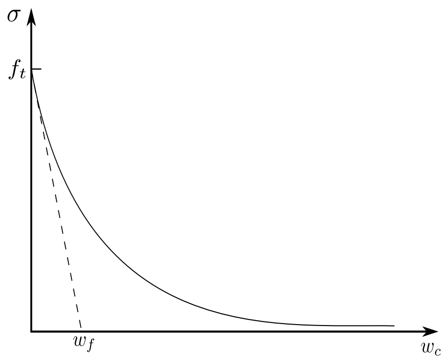

Figure 2: Stress crack-opening curve in uniaxial tension.

Under uniaxial tension, the exponential stress-crack opening curve shown in Figure 2 is obtained. For tension, α is modeled based on the expressions reported in CEB-FIP Model Code 2010 [3]. Thus,

$$\alpha = \begin{cases} 1 & \text{for } \dot{\tilde{\varepsilon}} \leq \dot{\varepsilon}_1 \\ \left(\dfrac{\dot{\tilde{\varepsilon}}}{\dot{\varepsilon}_1}\right)^{0.018} & \text{for } \dot{\varepsilon}_1 \leq \dot{\tilde{\varepsilon}} \leq \dot{\varepsilon}_2 \\ 0.0062\left(\dfrac{\dot{\tilde{\varepsilon}}}{\dot{\varepsilon}_1}\right)^{1/3} & \text{for } \dot{\varepsilon}_2 \leq \dot{\tilde{\varepsilon}} \end{cases} \tag{5}$$

where $\dot{\varepsilon}_1 = 1 \times 10^{-6}\ \mathrm{s}^{-1}$ and $\dot{\varepsilon}_2 = 10\ \mathrm{s}^{-1}$.

In order to circumvent mesh dependency, the rate factor α is made a function of displacement rate instead of the strain rate once damage is initiated:

$$\frac{\tilde{\varepsilon}^{n} - \tilde{\varepsilon}^{n-1}}{t^{n} - t^{n-1}} = \beta h_{\mathrm{e}} \frac{\tilde{\varepsilon}^{n+1} - \tilde{\varepsilon}^{n}}{t^{n+1} - t^{n}} \tag{6}$$

The parameter β is determined at the onset of the damage and remains unchanged thereafter. Furtheremore, $n+1$ is the first step where damage is nonzero.

3 Analysis

The model was implemented in the OOFEM and a detailed mesh-dependence study was carried out in [6]. In this section describes the analysis of the modified Split Hopkinson Pressure Bar (SHPB) for which the experiments were conducted by [9]. The setup and geometry of the experiments is shown in Figure 3. The total length of the incident bar (made of aluminum) is 5500 mm. A 250 mm concrete specimen is bonded at the end of the incident bar. The section diameter of the incident bar and concrete specimen is 74.20 mm. The incident bar is impacted by a steel projectile. Three impact velocities were applied: 4.10 m/s, 7.60 m/s and 11.10 m/s. The projectile has the following properties: mass density $\rho = 7850$ kg/m^3, Young's modulus $E = 210$ GPa, Poisson's ratio $\nu = 0.33$. The incident bar has the following properties: mass density $\rho = 2720$ kg/m^3, Young's modulus $E = 72.7$ GPa, Poisson's ratio $\nu = 0.34$. The concrete specimen has the following properties: mass density $\rho = 2400$ kg/m^3, Young's modulus $E = 38.9$ GPa, Poisson's ratio $\nu = 0.18$. The uni-axial compressive strength is 43.2 MPa, the tensile strength is 3.24 MPa, the fracture energy is 125 N/m.

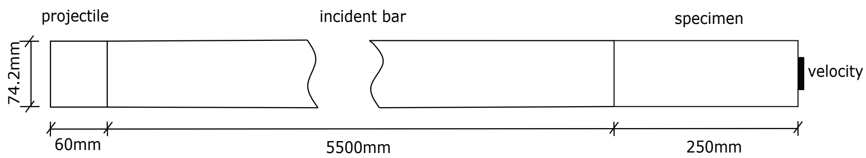

Figure 3: Geometry of the SHPB test set-up adapted from [9].

The incident bar and projectile are modelled to be linear-elastic. The strain rate dependent isotropic damage model is selected for the concrete specimen.
The velocity versus time figure for the point at the end of the concrete specimen is obtained under three different impact velocities, as shown in Figure 4. It can be seen from it, the higher the impact speed, the higher the particle velocity at the free end. In addition, when the time is 0.00126 s, the failure patterns of concrete specimens predicted by the numerical simulation are shown in Figure 4 as well. In this figure, concrete specimens are blue cylinders, and the shades of red indicates the magnitude of the maximum principal strain of the concrete. Here, the bright red corresponds to a strain of 0.01. It can be observed that the number of cracks in the analysis increases with increasing loading rate. This phenomenon is also reported in the experiment.

4 Conclusions

We introduced a strain rate dependent isotropic damage model. The results of our initial numerical simulations of the spall experiment show that the model can be used for the prediction of the response of concrete structures under high strain rates, because it is able to predict the increase in numbers of crack with increasing impact velocity. In the next steps, the numerical results will be compared in more detailed with the experimental observations. Also, the constitutive model for concrete will be extended to a damage-plasticity approach.

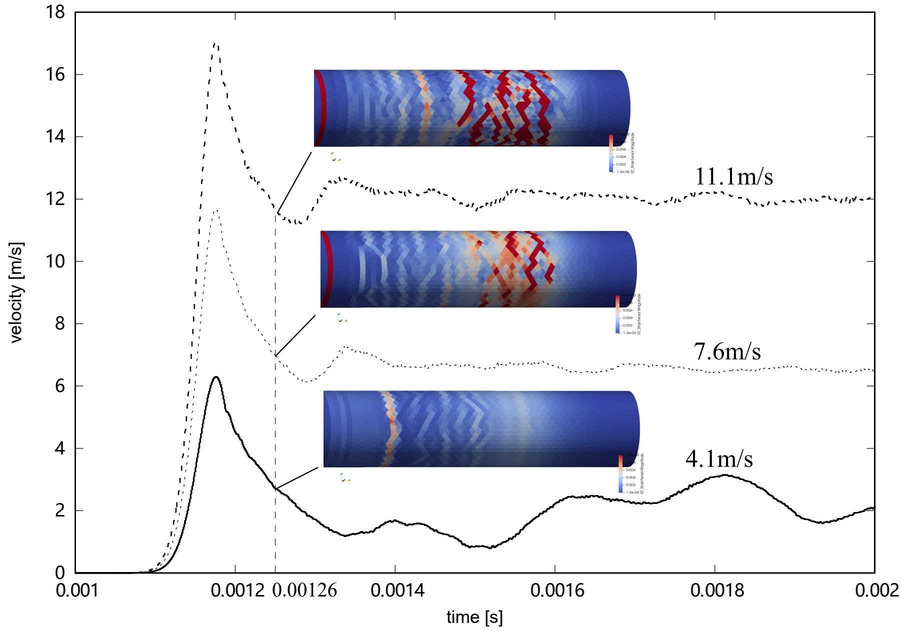

Figure 4: Particle velocities at the end and crack patterns of the concrete specimen for three impact velocities.

References

[1] Bažant, Z. P. and Jirásek, M. Nonlocal integral formulations of plasticity and damage: Survey of progress. *Journal of Engineering Mechanics, ASCE*, 128(10):1119–1149, 2002.

[2] Bažant, Z. P. and Oh, B.-H. Crack band theory for fracture of concrete. *Materials and Structures*, 16:155–177, 1983.

[3] CEB-FIP. *CEB-FIP Model Code 2010, Design Code*, 2012.

[4] Jirásek, M. and Bauer, M. Numerical aspects of the crack band approach. *Computers and Structures*, 110–111:60–78, 2012.

[5] Li, Q. M.; Reid, S. R.; Wen, H. M., and Telford, A. R. Local impact effects of hard missiles on concrete targets. *International Journal of Impact Engineering*, 32(1-4):224–284, 2005.

[6] Liu, X.; Lee, C. H., and Grassl, P. On the modelling of the rate dependence of strength using a crack-band based damage model for concrete. In *Proceedings of Euro-C*. Taylor and Francis, 2022.

[7] Patzák, B. OOFEM – An object-oriented simulation tool for advanced modeling of materials and structure. *Acta Polytechnica*, 52:59–66, 2012.

[8] Piani, T. Li; Weerheijm, J., and Sluys, L. J. Dynamic simulations of traditional masonry materials at different loading rates using an enriched damage delay: Theory and practical applications. *Engineering Fracture Mechanics*, 218:106576, 2019.

[9] Schuler, H.; Mayrhofer, C., and Thoma, K. Spall experiments for the measurement of the tensile strength and fracture energy of concrete at high strain rates. *International Journal of Impact Engineering*, 32(10):1635–1650, 2006.